DALTON
FULL PAPER

EPR Measurements corroborate information concerning the nature of $(H_2O)_5Cr^{III}$–alkyl complexes

Nurit Shaham,[a] Haim Cohen,[ab] Dan Meyerstein[ac] and Eckhard Bill[d]

[a] *Chemistry Department, Ben-Gurion University of the Negev, Beer-Sheva, Israel*
[b] *Nuclear Research Centre Negev, Beer-Sheva, Israel*
[c] *The College of Judea and Samaria, Ariel, Israel*
[d] *Max-Planck-Institut für Strahlenchemie, Stiftstr. 34–36, D-45470 Mülheim/Ruhr, Germany*

Received 12th June 2000, Accepted 18th July 2000

The X-band EPR spectra of $[(H_2O)_5Cr^{III}–CHCl_2]^{2+}$, $[(H_2O)_5Cr^{III}–CHCBr_2]^{2+}$, $[(H_2O)_5Cr^{III}–CH_3]^{2+}$, $[(H_2O)_5Cr^{III}–CH_2CO_2H]^{2+}$ and $[(H_2O)_5Cr^{III}–CH(CH_3)OC_2H_5]^{2+}$ were measured at liquid helium temperatures. For all complexes the major derivative signal is observed at $g'_{perp} \approx 4$ with weaker signals at $g'_{par} \approx 2$ and $g' \approx 5.9$. The signals broaden with increasing temperature and can not be observed at $T \geq 20$ K. the low-temperature spectra could readily be simulated by using the spin Hamiltonian formalism for $S = 3/2$ with axial and rhombic zero-field splitting parameters $D = -1.6$ cm^{-1} and $E/D = 0.06$, respectively. Based on these results the $(H_2O)_5Cr–R^{2+}$ complexes studied here are best described as chromium(III) compounds with a covalent chromium–carbon bond. In accord with expectations, this bond has a considerably larger covalent nature than the Cr–X bond, where X = halide, *etc*.

Introduction

A large variety of complexes of the type $[(H_2O)_5Cr^{III}–CR^1R^2R^3]^{2+}$ have been prepared.[1] Their spectroscopic[1,2] and chemical properties[1,3] are in accord with a central trivalent chromium cation. However some properties indicate that the chromium–carbon bond in these complexes has a more covalent nature than that observed in Werner type $(H_2O)_5CrX^{2+}$ complexes. Thus observations indicate: (1) many of these complexes decompose in the absence of an excess of $Cr(H_2O)_6^{2+}$, *via* homolysis of the metal–carbon σ bond,[1a,4] eqn. (1); this

$$(H_2O)_5Cr^{III}–CR^1R^2R^3 \rightleftharpoons Cr(H_2O)_6^{2+} + {}^{\bullet}CR^1R^2R^3 \quad (1)$$

phenomenon is, at least in part, due to the reducing properties of the formally carbanion ligands; (2) the ligands $^{-}$**:**$CR^1R^2R^3$ induce a strong *trans* effect, *i.e.* the rate of ligand exchange in the *trans* position is orders of magnitude higher than that in Werner type $(H_2O)_5CrX^{2+}$ complexes;[5] (3) it was proposed[1b,2] that the relatively large absorption coefficients of the d–d transitions at ≈400 nm are due to a partial mixing with a charge transfer process.

It was noted some time ago that no EPR signal at $g \approx 2$ is observed for the $(H_2O)_5Cr^{III}–CH_2CO_2H^{2+}$ complex in aqueous solution at 295 K as well as in frozen samples at 77 K. Furthermore the kinetics of the heterolysis reaction (2) could be

$$(H_2O)_5Cr^{III}–CH_2CO_2H^{2+} \xrightarrow{H_3O^+} Cr(H_2O)_6^{3+} + CH_3CO_2H \quad (2)$$

followed by the appearance of the EPR signal due to $Cr(H_2O)_6^{3+}$.[6] However strong EPR signals are observed for the Werner type complexes $Cr(H_2O)_6^{3+}$ and $(H_2O)_5CrX^{2+}$, where X = halide or a similar anion.[1a,b] It seemed therefore of interest to study in detail the origin of this difference in the EPR properties of these complexes. For this purpose the EPR spectra of several $[(H_2O)_5Cr^{III}–CR^1R^2R^3]^{2+}$ complexes were measured at liquid helium temperatures.

Experimental

Materials

A. R. grade chemicals were used. Solutions were prepared with triply distilled water. The complexes $[(H_2O)_5Cr^{III}–CHCl_2]^{2+}$ and $[(H_2O)_5Cr^{III}–CHBr_2]^{2+}$ were synthesized by mixing an excess of $Cr(H_2O)_6^{2+}$ in aqueous solutions at pH 1.0 with chloroform or bromoform dissolved in acetone. In these solutions reactions (3) and (4) occur.[7] The complexes were separated on a Dowex

$$[Cr(H_2O)_6]^{2+} + CHX_3 \longrightarrow [(H_2O)_6Cr^{III}–X]^{2+} + {}^{\bullet}CHX_2 \quad (3)$$

$$[Cr(H_2O)_6]^{2+} + {}^{\bullet}CHX_2 \longrightarrow [(H_2O)_6Cr^{III}–CHX_2]^{2+} \quad (4)$$

50X cation exchange column with 1 M $NaClO_4$ as the eluent. The solution of the complexes $[(H_2O)_5Cr^{III}–CHCl_2]^{2+}$, $[(H_2O)_5Cr^{III}–CHBr_2]^{2+}$ contained $(1–6) \times 10^{-3}$ M of the complex, 1 M $NaClO_4$ and low concentrations of $Cr(H_2O)_6^{3+}$ in the pH range of 3.0–3.5. The complexes $[(H_2O)_5Cr^{III}–CH_3]^{2+}$, $[(H_2O)_5Cr^{III}–CH_2CO_2H]^{2+}$ and $[(H_2O)_5Cr^{III}–CH(CH_3)OC_2H_5]^{2+}$ were synthesized using the radiation chemistry technique. Solutions containing 0.30 M RH, 1×10^{-3} M $Cr(H_2O)_6^{2+}$ at pH 3 were irradiated with 2500 Gray in the Van der Graaf electron accelerator of the Max-Planck-Institut für Strahlenchemie in Mülheim/Ruhr, Germany. Under these conditions reactions (5),[8] (6),[9] (7),[10] (8),[11] (9),[1c] and (10),[1b] have to be

$$H_2O \xrightarrow{e^-} {}^{\bullet}OH, e^-_{aq}, {}^{\bullet}H, H_2, H_2O_2 \quad (5)$$

$$H_3O^+ + e^-_{aq} \longrightarrow {}^{\bullet}H \quad (6)$$

$$CH_3CO_2H/(C_2H_5)_2O + {}^{\bullet}OH/{}^{\bullet}H \longrightarrow {}^{\bullet}CH_2CO_2H/{}^{\bullet}CH(CH_3)OC_2H_5 + H_2O/H_2 \quad (7)$$

$$(CH_3)_2SO + {}^{\bullet}OH \longrightarrow {}^{\bullet}CH_3 + CH_3SO_2H \quad (8)$$

$$H^{\bullet} + Cr(H_2O)_6^{2+} \longrightarrow [(H_2O)_5Cr^{III}–H]^{3+} \longrightarrow Cr(H_2O)_6^{3+} + H_2 \quad (9)$$

DOI: 10.1039/b004755o

$$\mathrm{Cr(H_2O)_6}^{2+} + {}^{\bullet}\mathrm{CR^1R^2R^3} \longrightarrow [\mathrm{(H_2O)_5Cr^{III}{-}CR^1R^2R^3}]^{2+} \quad (10)$$

considered. These solutions were used without any further purification. Solutions contained (1–5) × 10^{-4} M of the desired complex, 0.3 M RH, (3–8) × 10^{-4} M $\mathrm{Cr(H_2O)_6}^{3+}$ and were in the pH range of 1.0–3.0.

X-Band EPR spectra were recorded on a Bruker ESP 300E spectrometer equipped with a helium flow cryostat (Oxford Instruments ESR 910), an NMR field probe (Bruker 035M and a microwave frequency counter HP5352B). Spin-Hamiltonian simulations of the EPR spectra were performed with a program which was developed from the $S = 5/2$ routines of Gaffney and Silverstone[12] and which specifically makes use of the resonance-search procedure based on a Newton–Raphson algorithm as described therein. Frequency- and angular-dependent contributions to the linewidths were considered in the powder simulations.[13] The line shapes of the spin packets were either Lorentzian or Gaussian, derivative or absorption lines, depending on the type of spectra. We did not consider hyperfine splitting terms for ^{53}Cr nuclei ($I = 3/2$, 9.8% natural abundance) which can be neglected due to the broad experimental lines. The simulations are based on the spin Hamiltonian for the electronic spin ground state multiplet, eqn. (11), where S is the spin of the multiplet (3/2) and D and

$$H = D[S_z^2 - \tfrac{1}{3}S(S+1) + (E/D)(S_x^2 - S_y^2)] + \mu_B BgS \quad (11)$$

E/D are the usual axial and rhombic zero-field parameters.[14] Distributions of E/D (or alternatively D) were taken into account by summation of a series of powder spectra calculated at distinct values of that parameter, with weight factors taken from the Gaussian distribution. Usually twenty spectra were superimposed in this procedure. The distribution parameter was equidistantly sampled in the range ±3 of the Gaussian distribution.

Results and discussion

The complexes with a chromium–carbon σ bond $[\mathrm{(H_2O)_5Cr^{III}{-}CHCl_2}]^{2+}$ and $[\mathrm{(H_2O)_5Cr^{III}{-}CHBr_2}]^{2+}$ show distinct X-band spectra which were measured in frozen solution at liquid helium temperatures, as shown in Fig. 1A,B. For both samples a prominent derivative signal is observed at $g'_{\mathrm{perp}} \approx 4$ and a trough at $g'_{\mathrm{par}} \approx 2$. The pattern at $g'_{\mathrm{par}} \approx 2$ is superimposed by an additional derivative line that originates from residual amounts of $\mathrm{Cr(H_2O)_6}^{3+}$ ions in the solution, as can be inferred from a comparison with the spectrum of intentionally made $\mathrm{Cr(H_2O)_6}^{3+}$ in analogous solutions and measured under the same conditions (Fig. 2A). Double integration of both types of spectra reveals a contamination contribution of up to 20% of $\mathrm{Cr(H_2O)_6}^{3+}$ in the samples of $[\mathrm{(H_2O)_5Cr^{III}{-}CHCl_2}]^{2+}$ and $[\mathrm{(H_2O)_5Cr^{III}{-}CHBr_2}]^{2+}$. In total we found about 0.9 spin per chromium ion in both samples. This was derived by double integration and comparison with a copper(II) standard. The intensity of the spectra decreased with increasing temperature according to the usual Curie–Weiss behaviour for $T \geq 5$ K. In addition the experimental signals were strongly attenuated by temperature-dependent line broadening; no spectra could be observed at temperatures above 20 K.

The effective g values $g \approx 4$ and 2 of the complexes with chromium–carbon σ bonds are typical of an electronic spin $S = 3/2$ with moderately large zero field splitting (ZFS) and small rhombicity ($D > h\nu \approx 0.3$ cm^{-1} at X-band; $E/D \approx 0$).[15] In this regime of ZFS the spin quartet is split into two Kramers doublets, |3/2, ±1/2> and |3/2, ±3/2>, for virtually all fields applied in the EPR spectrometer and EPR transitions occur only within these doublets. For $E/D = 0$ only the $m_s = \pm 1/2$ doublet is EPR detectable whereas the $m_s = \pm 3/2$ doublet is EPR silent. In this limiting case of large axial ZFS ($D \gg h\nu$, $E/D = 0$) the effective g values for |3/2, ±1/2> would be expected at $g_{\mathrm{perp}} = 2S + 1$ for fields applied in the x/y directions, and at $g_{\mathrm{par}} = 2$ along z, which is in close accordance to what is found experimentally for the powder samples (frozen solutions) of $[\mathrm{(H_2O)_5Cr^{III}{-}CHCl_2}]^{2+}$ and $[\mathrm{(H_2O)_5Cr^{III}{-}CHBr_2}]^{2+}$.

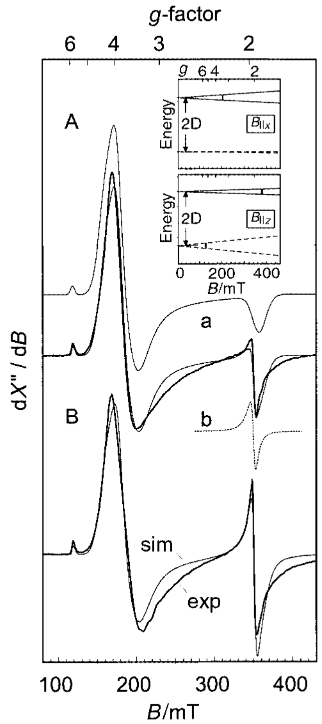

Fig. 1 (A) X-Band EPR spectra of $[\mathrm{(H_2O)_5Cr^{III}{-}CHCl_2}]^{2+}$. Experimental conditions: microwave frequency 9.6529 GHz, microwave power 100 μW, modulation amplitude 1.1 mT, temperature 7 K. The simulation (thin line) is a superposition of subspectra (a) and (b) with spin-Hamiltonian parameters for a: $D = -1.6$ cm^{-1}, $E/D = 0.057$, $\sigma(E/D) = 0.033$, $g = \{1.967, 1.967, 1.95\}$, Gaussian lines with frequency-dependent linewidth $W_f = 40$ mT and an additional angular-dependent contribution in the y direction $W_y = 18$ mT; b is a single-line approximation of the spectral contribution from 'free' chromium hexaaqua complexes with effective g value 1.98 (2% integral intensity). Inset: energies of the magnetic sublevels of the $S = 3/2$ manifold as a function of the field applied in the molecular x and z directions for $D = -1.6$ cm^{-1}, $E/D = 0.06$. (B) X-Band EPR spectrum of $[\mathrm{(H_2O)_5Cr^{III}{-}CHBr_2}]^{2+}$. Experimental conditions: microwave frequency 9.6545 GHz, microwave power 100 μW, modulation amplitude 1.1 mT, temperature 5 K. The simulation is a superposition of the subspectra a and b as described for (A), but with $W_f = 50$ mT, $W_y = 0$ for a and 12% intensity for b.

In the first order perturbation approximation, a finite value of the rhombicity parameter leads to a splitting of g_x' and g_y' according to $E/D = 1/12(g_y' - g_x')$. Since the experimental spectra do not show a resolved splitting of the pattern at $g' \approx 4$ one can take the overall width of the line at $g' \approx 4$ to obtain a rough estimate for the upper limit of E/D of about 0.06. The actual values of the ZF parameters of $[\mathrm{(H_2O)_5Cr^{III}{-}CHCl_2}]^{2+}$ and $[\mathrm{(H_2O)_5Cr^{III}{-}CHBr_2}]^{2+}$, which describe the electronic structure of the chromium complexes, could readily be determined from spin-Hamiltonian simulations of the EPR spectra by using the full matrix approach. The simulations showed that the experimental line shape can not be reproduced by a single $S = 3/2$ species with a well defined value for E/D, even if one employs angular dependent line shape distributions of the type $W^2 = (\Sigma W_i^2 l_i^2)^{\frac{1}{2}}$, where l_i denotes the direction cosines of the applied field. Particularly also the intensity of the well resolved, narrow small peak at about $g' = 5.9$ is considerably underestimated, if E/D is 0.06 as derived above from the absence of splitting of the powder line at $g' = 4$. The weak signal at $g' = 5.9$ results from an almost forbidden "$\Delta m = 3$" transition within the $m_s = \pm 3/2$ Kramers doublets, as indicated in the inset of Fig. 1A. The line gains some intensity due to level mixing of $m_s = \pm 3/2$ and ±1/2 states for molecular orientations in the

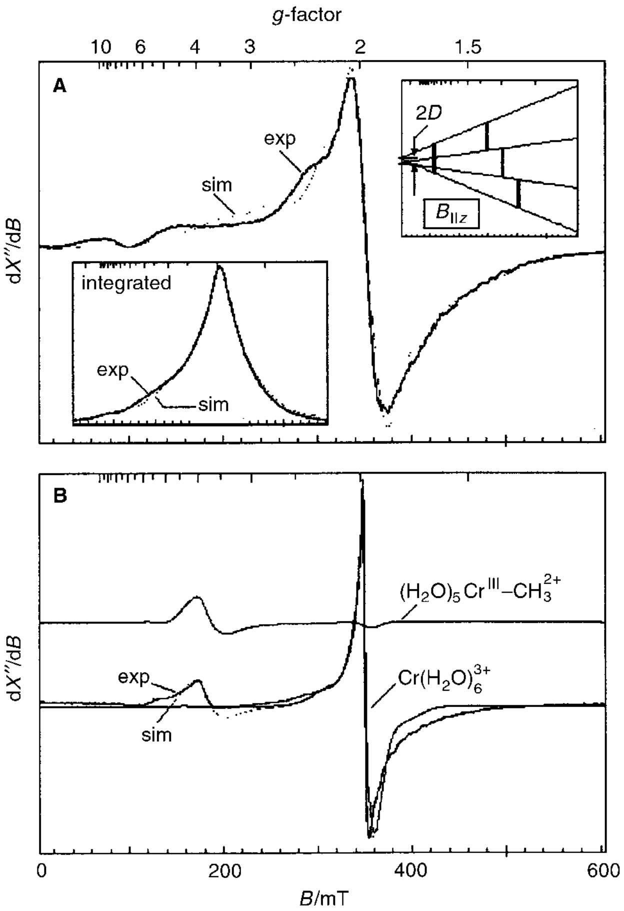

Fig. 2 (A) X-Band EPR spectra of $Cr(H_2O)_6^{3+}$. Experimental conditions: microwave frequency 9.6539 GHz, microwave power 200 μW, modulation amplitude 1.1 mT, temperature 5 K. Spin Hamiltonian simulation: $D = 0.071$ cm^{-1}, $E/D = 0.147$, $g = \{1.923, 1.99, 1.99\}$, Lorentzian lines with angular-dependent linewidths $W = \{34, 75.6, 66.6\}$ mT. Bottom inset: experimental absorption spectrum obtained by numerical integration and corresponding simulation with parameters as given above for the derivative spectrum. Top inset: energies of the magnetic sublevels of the $S = 3/2$ manifold as a function of the field applied in the molecular z direction for $D = 0.07$ cm^{-1}, $E/D = 0.15$. (B) X-Band EPR spectra of $[(H_2O)_5Cr^{III}–CH_3]^{2+}$. Experimental conditions: microwave frequency 9.6551 GHz, microwave power 200 μW, modulation amplitude 1.1 mT, temperature 5 K. Spin-Hamiltonian simulation: $D = 0.025$ cm^{-1}, $E/D = 0.157$, $\sigma(E/D) = 0.01$, $g = \{1.959, 1.959, 1.972\}$, Gaussian lines with angular-dependent linewidths $W = \{32, 32, 3\}$ mT.

frozen solution that have the applied field close to the z axis, if the ZFS is only moderately strong and if $E/D \neq 0$.[15] Therefore the appearance of this peak yields an upper limit for D and a lower limit for E/D. A satisfactory fit of the spectra could be obtained when D was negative and when we allowed for a distribution of E/D, which for the sake of simplicity was assumed to be Gaussian. With these assumptions an automatic optimization of the variables yielded $D = -1.6$ cm^{-1}, $E/D = 0.06$ and $\sigma(E/D) = 0.03$ (half width of the distribution). The negative value of the axial zero field parameter D means that the $|\pm 3/2>$ Kramers doublet is the ground state in the $S = 3/2$ mainfold and the major EPR intensity ($g = 4$ and 2) comes from an excited state (the $|\pm 1/2>$ doublet). The best values found for the intrinsic electronic g factors are $g = 1.97, 1.97, 1.95$, constrained to axial symmetry in the fit.

In order to check whether the halide substituents in the complexes $(H_2O)_5Cr^{III}–CHX_2^+$ have a significant influence on the EPR parameters the complexes $[(H_2O)_5Cr^{III}–CH_3]^{2+}$, $[(H_2O)_5Cr^{III}–CH_2CO_2H]^{2+}$ and $[(H_2O)_5Cr^{III}–CH(CH_3)OC_2H_5]^{2+}$ were synthesized. Their spectra, see for example $[(H_2O)_5Cr^{III}–CH_3]^{2+}$, Fig. 2B, clearly show that the bands at $g' = 4$ and 5.9 are due to the chromium–carbon σ bond. The spectra could satisfactorily be simulated with a superposition of two $S = 3/2$ subspectra due to (i) the contribution of the target complex $(H_2O)_5Cr^{III}CH_3^{2+}$ (36% integrated intensity) and (ii) a major contribution (64%) from residual $Cr(H_2O)_6^{3+}$ in the sample (see Experimental section). The contribution (i) from $(H_2O)_5Cr^{III}CH_3^{2+}$ has the characteristic features with strong signals at $g' = 4$ and 2 as described above for the halogenated Cr–C compound. Simulation parameters with large ZFS were taken from the corresponding subspectrum a shown in Fig. 1A. In contrast, the appearance of contribution (ii) is in qualitative accord with the spectrum observed for chromium(III) ions in water (Fig. 2A). For these systems the EPR transitions are centred around $g = 2$. Only a broad derivative band with some faint features at higher g values are measured from the frozen solutions. The features indicate the presence of small ZFS ($D < h\nu$). The ZF and Zeeman splittings of the $S = 3/2$ multiplet for such a system are depicted in the top inset of Fig. 2A, together with the corresponding EPR transitions for $B \| z$. The apparent width and the shape of the main experimental line is partially preparation-dependent. We presume that either weak intermolecular spin–spin interactions or variations in the average ligand field induced by strain in the frozen solutions are responsible for the disparity. We could simulate the variety of spectra by using ZFS $|D| < 0.1$ cm^{-1} (the sign can not be determined), moderate rhombicity $E/D = 0.15$ and anisotropic linewidths as common features. Distributions of D or E/D did not improve the overall quality of the fits for the hexaaquachromium(III) complex (Fig. 2A). This supposedly means that for the weak ZF interactions also the inhomogeneities are small and probably affect several parameters at the same time. The quality of the simulation by using inhomogeneous line broadening is demonstrated also for the absorption spectrum as shown in the bottom inset of Fig. 2A. This pattern is obtained by numerical integration of the experimental derivative spectrum and a simulation with absorption line shapes. The EPR contribution of $Cr(H_2O)_6^{3+}$ in the sample of $(H_2O)_5Cr^{III}CH_3^{2+}$, however, could be better reproduced with a distribution of E/D (=0.01) and a smaller average value $E/D = 0.025$ (Fig. 2B). It appears from the scattering of the parameters for this species in different samples that the actual ZFS of 'bare' Cr^{III} in water is not better determined than $|D| < 0.1$ cm^{-1}, which, however, is significantly different from the results for the complexes with Cr–C bonds.

The observation that the ZFS is considerably larger for the $[(H_2O)_5Cr^{III}–CR^1R^2R^3]^{2+}$ than for $Cr(H_2O)_6^{3+}$ and $(H_2O)_5CrX^{2+}$ complexes, where X = halide, *etc.*, points out that the $^-{:}CR^1R^2R^3$ ligands induce a larger crystal field splitting, *i.e.* the bond in these complexes has a larger covalent contribution. This finding is in accord with the visible spectra of these complexes where the d–d transitions are shifted to the blue by the alkyl ligands.[1a] The larger covalent contribution to the complexes with chromium–carbon σ bonds also explains the temperature effect on their EPR spectra. The spin–lattice interaction increases with the ZFS and therefore the signal "disappears" at relatively low temperatures.

The zero-field parameters are in accord with the values found for other chromium(III) co-ordination compounds[15,16] with the usual electronic configuration $(d_{xy})^1(d_{xz})^1(d_{yz})^1$ and spin $S = 3/2$. The small rhombicity observed is somewhat surprising for the complexes $[(H_2O)_5Cr^{III}–CR^1R^2R^3]^{2+}$ but is in accord with the slight rhombic distortion observed in the crystal structures of the analogous *trans*-(acac)$_2$LCr–R, where R = CH_2Cl or $CHCl_2$ and L = H_2O or $C_5H_5N_9$.[17] We take this observation as an indication that the electronic structure of Cr^{III} in these complexes is primarily determined by the σ-bonded carbon, and the other ligands play only a minor role for the "ligand field" experienced by the chromium valence orbitals.

Acknowledgements

This study was supported in part by a grant from the Budgeting and Planning Committee of the Council of Higher Education and the Israel Atomic Energy Commission. D. M. wishes to express his thanks to Mrs Irene Evens for her ongoing interest and support.

References

1 (*a*) J. H. Espenson, *Adv. Inorg. Bioinorg. Mech.*, 1982, **1**, 1; (*b*) H. Cohen and D. Meyerstein, *Inorg. Chem.*, 1974, **13**, 2434; (*c*) H. Cohen and D. Meyerstein, *J. Chem. Soc.*, *Dalton Trans.*, 1974, 2559.
2 A. Sauer, H. Cohen and D. Meyerstein, *Inorg. Chim. Acta*, 1989, **155**, 101.
3 W. Schmidt, J. H. Swinehart and H. Taube, *J. Am. Chem. Soc.*, 1971, **93**, 1117.
4 G. W. Kirker, A. Bakac and J. H. Espenson, *J. Am. Chem. Soc.*, 1982, **104**, 1249.
5 A. Bakac, J. H. Espenson and L. P. Miller, *Inorg. Chem.*, 1982, **21**, 1557; W. R. Bushey and J. H. Espenson, *Inorg. Chem.*, 1977, **16**, 2772.
6 H. Cohen and D. Meyerstein, unpublished work.
7 D. Dodd and M. D. Johnson, *J. Chem. Soc. A*, 1968, 34.
8 L. M. Dorfman and M. S. Matheson, *Pulse Radiolysis*, MIT Press, Cambridge, 1969.
9 L. M. Dorfman and I. A. Taube, *J. Am. Chem. Soc.*, 1963, **85**, 2370.
10 M. Ebert, J. P. Keene, A. J. Swallow and J. H. Baxendale, *Pulse Radiolysis*, Academic Press, New York, 1965; P. Neta, G. R. Holdern and R. H. Schuler, *J. Phys. Chem.*, 1971, **75**, 449; A. Appleby, G. Scholes and M. Simic, *J. Am. Chem. Soc.*, 1963, **85**, 3891.
11 D. Vietwisch, E. Janata and K. D. Asmus, *J. Chem. Soc.*, *Perkin Trans. 2*, 1980, 146.
12 B. J. Gaffney and H. J. Silverstone, in *Biological Magnetic Resonance*, eds. L. J. Berliner and J. Reuben, Plenum Press, New York, London, 1993, vol. 13.
13 J. R. Pilbrow, *Transition Ion Electron Paramagnetic Resonance*, Clarendon Press, Oxford, 1990.
14 A. Abragam and B. Bleany, *Electron Paramagnetic Resonance of Transition Ions*, Oxford University Press, Oxford, 1970.
15 F. E. Mabbs and D. Collison, *Electron Paramagnetic Resonance of d Transition Metal Compounds*, Elsevier, Amsterdam, 1992.
16 E. Pedersen and H. Toftlund, *Inorg. Chem.*, 1974, **13**, 1603; L. S. J. Singer, *Chem. Phys.*, 1955, **23**, 379.
17 Y. Abe and H. Ogino, *Bull. Chem. Soc. Jpn.*, 1989, **62**, 56.